A Frequency Addressable Ultrasonic Microfluidic Actuator Array

Ville Kaajakari, Abhijit Sathaye, and Amit Lal
*Sonic*MEMS Laboratory, Department of Electrical and Computer Engineering
University of Wisconsin-Madison, 1415 Engineering Drive, Madison, WI 53706, USA

ABSTRACT

In this paper, a microfluidic ultrasonic multi-actuator paradigm is introduced. Mixing, pumping, and particle capture are achieved by actuating polysilicon center-anchored circular plates and polysilicon sidewall cantilevers at ultrasonic frequencies using a single piezoelectric PZT (Lead Zirconate Titanate oxide) plate. Frequency addressability of acoustic streaming at surface microstructures is demonstrated by driving the bulk structure at the microstructure resonance frequencies. The actuator array is placed inside a microfluidic channel with a Reynold's number of approximately 0.1. Standing and rotating mode shapes of the polysilicon structures have been observed using an optical interferometer in the frequency range of 200 kHz to 10 MHz. Frequency dependent fluid motion was qualitatively deduced and experimentally verified using dimensional analysis of micro-acoustic-streaming.

Keywords: polysilicon plate, microfluidic, acoustic streaming

INTRODUCTION

Acoustic streaming in microfluid mixing and pumping has several attractive features compared to the other techniques to actuate the fluid in microchannels. For example, the stress waves responsible for acoustic streaming can be excited far away from the channel eliminating the need to integrate electrodes in close proximity to the channel. Other methods such as electro-osmosis, electrohydrodynamic pumping, magneto-hydrodynamic pumping, electrophoretic pumping need electric fields in the liquid requiring the liquid to be electrically conductive. In contrast, acoustic streaming based ultrasonic pumps or mixers are far less sensitive to electrical or chemical properties of the fluid. Thermal and piezoelectric bimorph pumps are based on large mechanical displacement of the fluid [1], whereas in acoustic streaming, the displacements are very small ($\sim$nm) but the high frequency results in high particle velocities. Recently many investigators have utilized acoustic streaming in microsystems [2–7]. A common trend in these investigations is the use of bulk micromachined SiN membranes or bulk silicon excited by piezoelectric thin films.

In this paper a bulk piezoelectric PZT plate is used to impart ultrasonic energy to the surface micromachined polysilicon structures placed inside a microfluidic channel. The ultrasonic vibrations applied to PZT/Si laminate are coupled to the surface micromachines via inertial drive and elastic deformation at the anchor (Figure 1). We have previously used this approach for microengine actuation and surface micro-

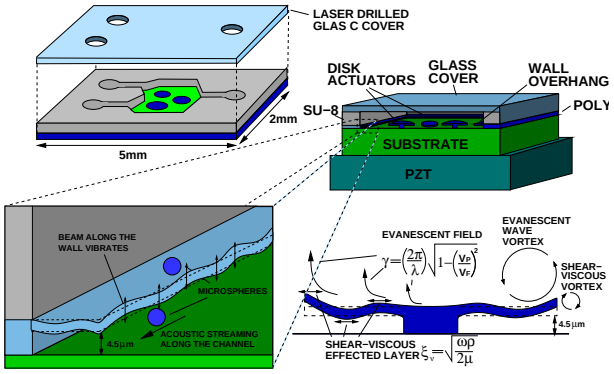

Figure 1. *A schematic of the microfluidic actuator*

machine assembly [8, 9]. Since the actuation is done from the back of the silicon die using a PZT plate, the need for any electrical connections near or inside the channel is eliminated. This gives interconnect free actuation of micromachines simplifying the channel sealing and electrical isolation. While the entire substrate is vibrated, the resonances of the surface micromachined structures amplify the motion producing larger acoustic field gradients. Furthermore, the nonlinear characteristic of acoustic streaming amplifies the effect of larger amplitudes on fluid motion. Hence, substantial fluid motion is observed in the vicinity of the resonating structures.

PRINCIPLE OF OPERATION

Substrate Resonances

The measured PZT/Si laminate electrical impedance and mode classes are shown in Figure 2. For frequencies less than 1 MHz flexural (bending) and longitudinal modes are dominant. Above 1 MHz the vibration energy is mostly in thickness type modes. In general the mode shapes are not complicated and simple analytical solutions do not exist. However, the modes are worth investigating due to the simplicity and potential low cost of the PZT/Si laminate.

Surface Micromachine Vibrations

Resonating surface micromachines are used to introduce additional vibrations and acoustic field gradients in the microfluid channels. The microstructures are actuated by exciting the PZT/Si laminate at frequencies coinciding with the microstructure resonance frequencies. In this paper, we focussed on center anchored disk and sidewall actuators shown in Figure 1.

To characterize the disk resonances, a phase-locked diode laser interferometer and a CCD camera was used. This interferometric visualization was done in vacuum ($<$100mTorr) to eliminate the viscous air damping. An example of a disk resonance with a five fold radial symmetry

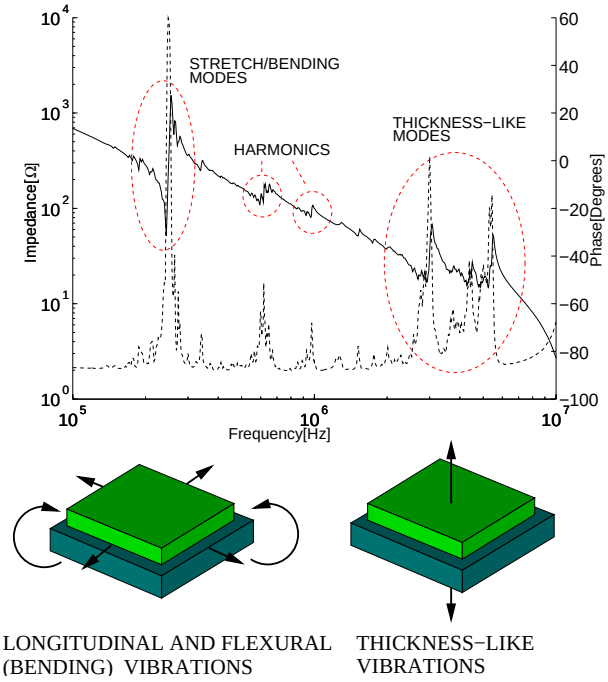

Figure 2. *The measured PZT/Si laminate electrical impedance and corresponding mode classes*

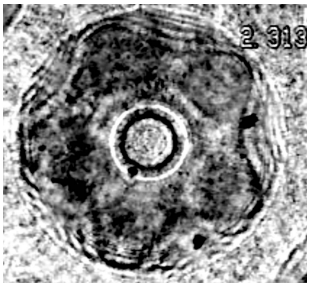

Figure 3. *Resonance mode having five nodes of a 1.15 µm thick polysilicon circular plate with a 500 µm outer diameter, 100 µm inner diameter at 231 kHz*

is shown in Figure 3. The vibration amplitude was as high as 2.5 μm measured by counting the fringes. In addition to the standing wave patterns, rotating modes (θ-directed traveling waves) of anchored disks were also excited. These rotating modes appeared at the frequency slightly off the fundamental standing mode resonance and showed a frequency hysteresis associated with the non-linear spring constants, and are currently under investigation.

ACOUSTIC STREAMING

Acoustic streaming can be attributed to the nonlinear convective mass transport due to gradients in acoustic fields. Nyborg and others have used the method of successive approximation to derive an effective force field due to acoustic gradients that move the liquid [10]. This force field is of the type

$$F = -\rho\langle v_a \cdot \nabla v_a \rangle, \qquad (1)$$

where v_a is the acoustic velocity field calculated using linear acoustic methodologies. The force field derived from Eq. 1 is used in the creeping flow equation to obtain the acoustic streaming flow pattern. The boundary motion due the presence of a transducer also gives rise to a flow due to boundary nonlinearity but is not important when the transducer displacement is much smaller than the device dimensions [11].

The solutions to the linear acoustic problem for complicated structures in microfluidic channels is analytically intractable. Numerical FEM solutions are possible for the linear acoustic problem. FEM modeling is required both at the micron and the millimeter scale requiring very high mesh densities. However, useful intuition of device operation can be obtained by studying classes of acoustic streaming. In fact, the microfluidic channel filled with microstructures driven at a widely varying range of frequencies provides an interesting test case to categorize acoustic streaming flows. A vibrating surface, much smaller than the acoustic wavelength, generates local vortices resulting in "microstreaming," a term coined by Nyborg. For example, a wire vibrating transversely results in vortices, a longitudinal actuator results in vortices [10]. Oscillating spheres result in vortices as well [12]. In cases where the device size is larger than the acoustic wavelength, gradients of the acoustic field over wavelength can also lead to vortices and linear flow. In the "microfluid actuation" section, five microscale lengths are identified as key parameters for dimensional analysis. They are the acoustic wavelength, the shear viscous depth, the evanescent decay length, the plate-substrate gap, and the channel height.

DEVICE FABRICATION

The process flow for the device fabrication is shown in the Figure 4. The steps are as follows :

1. Anchoring: 4.5 μm thick oxide layer was grown by successive LPCVD polysilicon depositions and thermal oxidations. The center anchor for the disk structures was created by lithographic patterning followed by the oxide etch using 6:1 BOE. The high thickness of oxide ensured that the final circular disk structures did not get stuck to the substrate during the release and that the 2 μm diameter polystyrene balls used to visualize the fluid flow could go under and come out beneath the disk without getting stuck.

2. Polysilicon deposition and patterning: After creating the anchors, a 1.2 μm polysilicon deposition was done at 580 ^{o}C and followed by a 900 ^{o}C stress anneal. The polysilicon disks and walls were then patterned by a RIE etch.

3. Cap fabrication: SU-8 walls with glass cover on top were fabricated by first removing oxide around the disk actuators with 6:1 BOE etch. Next 50 μm thick SU-8 coating was spun and patterned. The stress related problems resulting in poor adhesion of SU-8 to the substrate were solved by avoiding high thermal stresses. After SU-8 patterning, the disk actuators were released with 49 % HF etch (Figure 5). Finally 5 μm thick layer of SU-8 was used to bond the glass cap with laser drilled orifices on top of the channel serving as the entry point for the pipes used for injecting fluid into the channel.

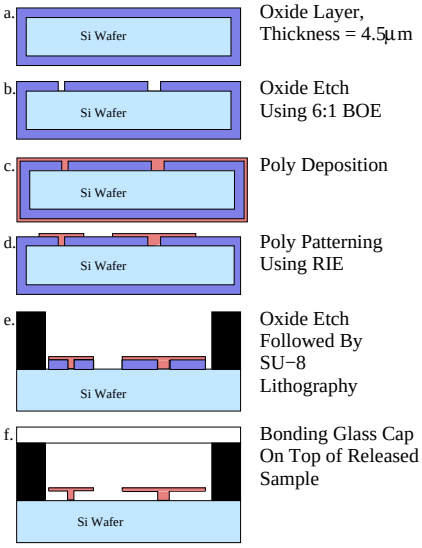

Figure 4. *The device fabrication process*

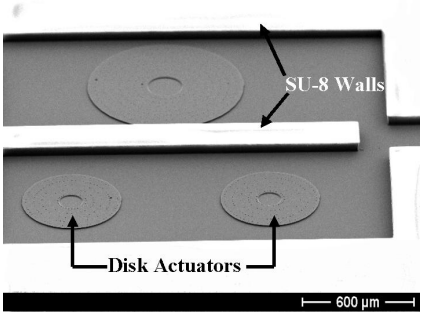

Figure 5. *SEM of fabricated device showing released polysilicon disks and SU-8 walls*

4. PZT bonding: The released and capped sample was adhesively bonded to a piezoelectric plate (PZT-4H, Lead-Zirconate-Titanate) using cyanoacrylate.

MICROFLUID ACTUATION

In this section, experimental fluidic results are discussed. In all experiments, the PZT was actuated with a 10 V peak-to-peak amplitude (when driving a 50 Ω load). The actual voltage across the PZT varied due to the frequency dependency of the PZT impedance and was less than 10 V. The observations were made with an optical microscope and the fluid motion was visualized with 2 μm polystyrene spheres.

Addressable Actuation

1. Substrate flexural resonances.
For frequencies less than 1 MHz, the fluid actuation is controlled by the flexural modes and the location of the disk actuators inside the channel. The structural dimensions of the surface microactuators are much smaller than the acoustic wavelength (1.5-7.5 mm for 0.1-1 MHz drive), and the microstructure acts as a scattering dipole source resulting in large vortices as shown in Figure 6.
Fluid vortices in the channel at locations other than the microstructures were also observed near the polystyrene bead clusters. These 10-30 μm clusters are believed to act as a scattering source in the same way as the disk actuators.

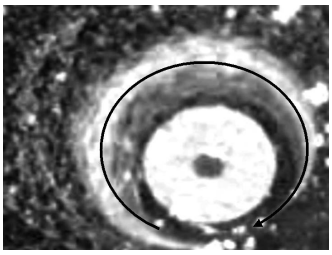

Figure 6. *Vortex formation around a disk actuator*

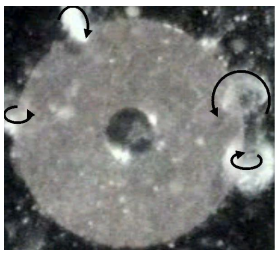

Figure 7. *Vortices along the disk periphery*

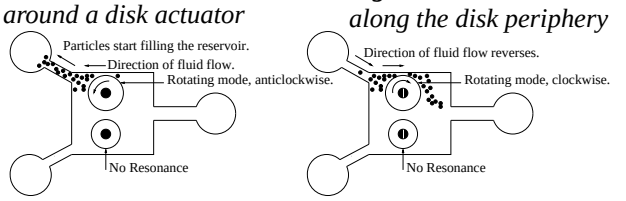

Figure 8. *Effect of resonance mode on direction of fluid flow*

2. Thickness mode substrate resonances. At frequencies between 1-10 MHz, the vibration energy is mainly in the thickness modes. At these frequencies, the acoustic wavelength is approximately ∼150-1500 μm. Another important length scale is the evanescent field decay length, which is the extent of a non-propagating acoustic field in the fluid because the flexural plate wave phase velocity is smaller than the fluid acoustic velocity [6]. The evanescent decay length at the 3-5 MHz frequency range is 30-50 μm. Using a dimensional argument, the near unity device-to-wavelength ratio and the near unity channel-height-to-evanescent-decay-length ratio implies acoustic field variation both in the vertical and radial directions in the vicinity of the circular plate.
These disk actuators can be used to amplify motion by *selectively* resonating them in the frequency range discussed above. It is possible to control fluid motion by frequency addressing the disk actuators. As an example, rotating modes caused microspheres to travel around the disk at velocities exceeding 7000 μm/s.
The rotating modes were used for bidirectional pumping as illustrated in Figure 8. With the excitation of anti-clockwise rotating mode, the polystyrene balls moved to the left filling the reservoir. As the reservoir fills up with the liquid, the increased pressure slows the actuated fluid flow. The Figure 9 shows the drop in velocity with time. By changing the drive frequency, a clockwise rotating mode is excited that pumps the liquid in the opposite direction. The flow direction could be changed repeatedly.

Edge Vortices

Microfluidic vortices formed along the periphery of the polysilicon disk actuators are shown in Figure 7. These vortices effectively trap the microspheres passing by the disk. This effect can be used for filtering, mixing, collecting, and accumulating particles.

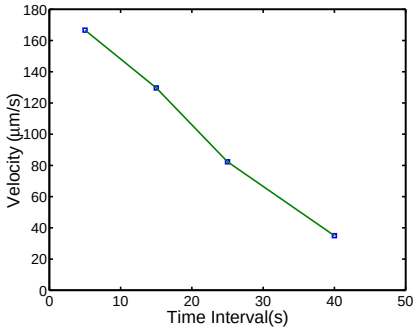

Figure 9. *The measured particle velocity variation with time for the flow in Figure 8*

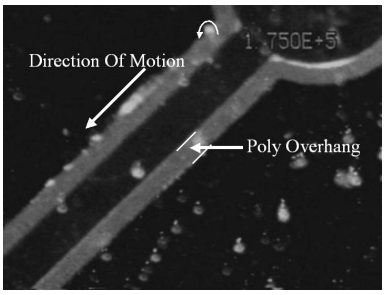

Figure 10. *Microsphere motion along the polysilicon overhang (∼50 µm)*

The edge vortex formation can be explained by plate edge shear viscous coupling into the fluid as shown in Figure 1. The shear viscous depth is $\sqrt{\nu/\omega}$, where ν is the the length scale over which the shear motion is coupled to the fluid. Here, ν is the kinematic viscosity and ω is the frequency. This length ranges from 2 μm at 100 kHz to 0.2 μm at 10 MHz for water. Thus the shear viscous depths being of the same order as the plate thickness and the plate substrate gap, implies large variants near the plate edges resulting in the observed edge vortices.

Fluid Pumping Along The Wall

The polysilicon sidewall excitation (500-600 kHz, 3-5 MHz) resulted in a traveling wave pattern of flexural waves along the wall of the channel with amplitude gradients at the corners. This effectively pumped the liquid along the wall edges as shown in Figure 10.

CONCLUSIONS

This paper investigated structures embedded in a fluidic channel with an approximate Re=0.1. The acoustic actuation was accomplished by a single PZT plate attached to the silicon die, a structure that is simple and potentially inexpensive as compared to other devices requiring thin piezoelectric films. Several fluid flows were observed in a wide frequency range of 200 kHz to 10 MHz. The resonances of the microstructures can be excited by the PZT actuator resulting in addressable excitation of structures with different resonance frequencies near the bulk resonances. This wide variation in frequency also allows one to study many kinds of fluid flows in which the microstructures can be modeled as point sources or distributed acoustic sources. The fluid motions include vortices and linear flow, which can be explained using dimensional analysis with the relevant length scales. These length scales include the acoustic wavelength, the evanescent wave decay length, the shear viscous depth, the channel height, and the structure-substrate gap. In addition to providing a framework to develop useful microfluidic devices, this paper provides future directions in optimization of vortex and linear flow actuation.

ACKNOWLEDGMENTS

We thank Wisconsin Center for Applied Microelectronics (WCAM) for device fabrication support. This work was funded by DARPA/MTO contract #F30602-00-2-0572.

REFERENCES

[1] P. Gravesen, J. Branebjerg, and O. Jensen, "Microfluidics - a Review", *Journal of Micromechanics and Microengineering*, vol. 3(4), pp. 168–182, Dec. 1993.

[2] R. Zengerle and H. Sandmaier, "Microfluidics", *Proceedings of the Seventh International Symposium on Micro Machine and Human Science*, pp. 13–20, 1996.

[3] A. Lal and R. White, "Ultrasonically Driven Silicon Atomizer and Pump", *Solid State and Actuator Workshop*, pp. 276–279, Hilton Head Island, USA, Jun. 3-6 1996.

[4] H. Wang and E. S. Kim, "Ejection Characteristics of Micromachined Acoustic-Wave Ejector", *The 10th International Conference on Solid-State Sensors and Actuators*, pp. 1784–1787, Sendai, Jun. 7-10 1999.

[5] P. Luginbuhl, S. D. Collins, G.-A. Racine, M.-A. Gretillat, N. F. de Rooij, K. G. Brooks, and N. Setter, "Flexural-Plate-Wave Actuators Based On PZT Thin Film", *Proceedings of the 10th Annual International Workshop on Micro Electro Mechanical Systems*, pp. 327–332, Nagoya, Japan, Jan. 26-30 1997.

[6] R. M. Moroney, R. M. White, and R. T. Howe, "Microtrasport Induced by Ultrasonic Lamb Waves", vol. 59(7), pp. 774–776, Aug. 1991.

[7] X. Zhu and E. S. Kim, "Microfluidic Motion Generation with Loosely-Focused Acoustic Waves", *The 9th International Conference on Solid-State Sensors and Actuators*, pp. 837–838, Chicago, USA, Jun. 16-19 1997.

[8] V. Kaajakari, S. Rodgers, and A. Lal, "Ultrasonicly Driven Surface Micromachined Motor", *Proceedings of the 13th Annual International Conference on Micro Electro Mechanical Systems*, pp. 40–45, Miyazaki, Japan, Jan. 23-27, 2000.

[9] V. Kaajakari and A. Lal, "Electrostatic Batch Assembly of Surface MEMS using Ultrasonic Triboelectricity", *Proceedings of the 14th IEEE International Conference on Micro Electro Mechanical Systems*, pp. 10–13, Interlaken, Switzerland, Jan 21-25, 2001.

[10] W. L. Nyborg, *Acoustic Streaming*, vol. 2B of *Physical Acoustics*, pp. 1415–1422, Academic Press, New York, 1949.

[11] C. E. Bradley, "Acoustic Streaming Field Structure: The Influence of the Radiator", *Journal of Acoustical Society of America*, vol. 100(3), pp. 1399–1408, Sep. 1996.

[12] N. Amin and N. Riley, "Streaming from a Sphere due to a Pulsating Source", *Journal of Fluid Mechanics*, vol. 210, pp. 459–473, Jan. 1990.